

Cite this: DOI: 10.1039/c0sm01220c

www.softmatter.org

Facile growth factor immobilization platform based on engineered phage matrices†

So Young Yoo, Anna Merzlyak and Seung-Wuk Lee*

Received 27th October 2010, Accepted 14th December 2010

DOI: 10.1039/c0sm01220c

Immobilized growth factors on tissue matrices play a critical role in controlling cell growth processes and cell morphology. We report a strategy for immobilizing growth factors on genetically engineered phage matrices for tissue regeneration. We modified M13 phages to express biotin-like peptides (HPQ) and/or integrin binding peptides (RGD) on their major and minor coat proteins. The resulting phages formed nanofibrous matrices that could easily immobilize growth factors FGFb and NGF. We demonstrated the synergistic roles of the growth factors and integrin binding peptides in controlling cell morphologies and growth. Our phage matrices, which can be easily functionalized with various ligands and growth factors, can be used as a convenient test bed for investigating the functions of various biochemical stimulants of numerous cell types.

Designing biomimetic materials with precisely controlled structural organization that closely mimics the natural tissue environment is critical for the development of regenerative medicine. In the body, cells are in close contact with neighboring cells and the extracellular matrix (ECM).^{1,2} The ECM is composed mainly of nanofibrous protein networks^{3–6} with fibrils that have diameters ranging between 3 and 20 nm.^{7–9} These nanofibrous structures, their mechanical stiffnesses, and various biochemical ligands provide instructive cues to nearby cells, dynamically orchestrating their morphologies and fates.^{10,11} The components of the ECM and the ligands bound to cell receptors provide chemical signalling to control cell behavior. The signals for adhesion, migration, proliferation and differentiation are provided by integrin binding, growth factors, and cytokine stimulation.^{12–15} These signalling motifs can be presented either directly upon contact or hidden and exposed only upon matrix remodelling or tissue injury.^{16–18} The matrix components can bind to soluble growth factor molecules from the physiological milieu and present them to cells as needed.^{19–21} Mimicking such complex and dynamic environments is challenging. We believe we can create a simplified cellular environment with preserved function by immobilizing effective growth factors. The use of immobilized growth factors has been

shown to have merits over the use of soluble growth factors. Immobilized EGF and insulin are known to prolong tissue stimulation effects.^{22,23} Sustained receptor activation by membrane-bound ligands or context-dependent growth factor and extracellular matrix (ECM) presentation are recognized to be important mechanisms for controlling stem cell fate.^{24,25} Presenting growth factors as part of an extracellular matrix, rather than just releasing them into the liquid medium, improves nerve regeneration and growth of smooth muscle cells during the engineering of artificial arteries.²⁶ However, the process of chemically modifying matrices to immobilize different growth factors is burdensome and often results in undesired changes to their physical and chemical structures. The development of a facile bioconjugation method for immobilizing chemical ligands with minimal change to the tissue scaffolds would, therefore, possess great merits for the development of novel tissue engineering materials.^{21,27,28}

The engineering of phages provides a novel toolkit for creating functional nanomaterials for the development of various applications in energy, electronics, and biomedical engineering.^{29–34} The previous use of engineered phages in biomedical applications has shown that phages effect little inflammation at targeted tissue sites.^{35,36} In addition, endocytosed phages in human tumor-derived cells and endothelial cells are degraded *via* the lysosomal pathway,^{37,38} a safe material clearance route for cell specific phages. Phages that have been modified to express RGD on their minor coat proteins have been used as vehicles to deliver therapeutic genes to target tissues and specific cancer imaging reagents.³⁹ Recently engineered filamentous phage has been used to construct novel tissue engineering matrices that exhibit desired functions.^{40–43} In particular, our group has used these engineered phages to construct nanofibrous materials that can self-assemble, self-replicate through bacterial infection, and have potential for use in several applications.^{40,41} Multiple signalling and therapeutic peptide motifs can be simultaneously displayed on the pIII, pVIII, and pIX protein coats of M13 phages through genetic modification.⁴⁴ Identical copies of the engineered phage can be easily reproduced in large scale through bacterial amplification, and the resulting phage can be used to construct two- and three-dimensional long-range ordered nanofibrous network structures without the use of microfabrication techniques. Therefore, phages may be good candidate materials for constructing versatile tissue matrices that can immobilize biochemical ligands and growth factors for the development of future regenerative medicines. Here, we report a facile growth factor immobilization strategy using novel phage-based tissue engineering matrices. We constructed phages to display biotin-like

1-220 Donner Lab, Bioengineering, University of California, Berkeley, Physical Biosciences Division, Lawrence Berkeley National Laboratory, Berkeley Nanoscience and Nanoengineering Institute, Berkeley, CA, 94720, USA. E-mail: leesw@berkeley.edu; Fax: +1-510-486-6488; Tel: +1-510-486-4628

† Electronic supplementary information (ESI) available: Detailed experimental sections. See DOI: 10.1039/c0sm01220c

peptides (His-Pro-Gln; HPQ) and/or integrin binding peptides (Arg-Gly-Asp; RGD) on their major and minor coat proteins. The resulting phages easily bound to streptavidin-conjugated FGFb and NGF, two growth factors for neural cells, and were able to stimulate and guide neural stem cells to proliferate and differentiate into desired morphologies. Our facile growth factor immobilization approach may be useful for studying biochemical cues in cell biology and creating future tissue engineering materials.

The engineered phages used in our study are presented in Fig. 1A and Table 1 (detailed methods for construction are provided in the ESI†). The HPQ motif allows binding to streptavidin-conjugated molecules, and the RGD motif promotes cell adhesion on the phage matrices. M13 phage is a filamentous bacterial virus (880 nm × 6.6 nm) that is covered mainly by 2700 copies of a major coat protein (pVIII) (Fig. 1A). pVIII covers ~98% of the viral surface and is spaced 2.7 nm apart, enabling a very dense and uniform peptide display. The pVIII is also readily available for protein binding interactions.⁴⁵ In addition, there are five minor coat proteins (pIII) at one end of the phage. Longer amino acid sequences can be inserted at the *N*-terminus of pIII (compared to pVIII) without compromising the structure or function of the phage.⁴⁶ The HPQ-peptide, which specifically binds to streptavidin, was previously identified by us and other research groups through phage display.^{47–50} Linear and circular HPQ motifs were found to have biotin-like specificity to streptavidin.^{51–53} We used both linear and circular HPQ motifs to genetically modify the pVIII and pIII phage coat proteins, respectively. We engineered the phage to display a relatively short linear peptide, FSHPQNT ($K_d = 125 \mu\text{M}$),^{51,54} on its major coat (HPQ8) to prevent interference with phage structure or propagation. We also engineered our phage to display a circular HPQ-peptide, C-HPQGPP-C ($K_d = 670 \text{ nM}$), on the five copies of pIII (HPQ3). The circular HPQ-peptide had a higher affinity for streptavidin than the linear HPQ-containing peptides.^{52,55} The inserted peptides were linked to a flexible glycine trimer to

Table 1 Genetically engineered functionalized pVIII and pIII phage^a

Name	pVIII	pIII
RGD8	<i>ADSGRGDTEDP</i>	
HPQ8	<i>AEFSHPQNTDP</i>	
HPQ3		<i>A-C-HPQGPP-C-GGGSAAE</i>
RGD8HPQ3	<i>ADSGRGDTEDP</i>	<i>A-C-HPQGPP-C-GGGSAAE</i>

^a Peptide inserts are shown in italic and bold. Functional sequences are also underlined.

give the peptides easier access to their binding receptors.^{21,56,57} We also inserted integrin binding peptides on the major coat proteins of phage that expressed HPQ on their pIII proteins (RGD8HPQ3). Through the HPQ sites, we were able to immobilize streptavidin-conjugated FGFb (strep-FGFb) and NGF (strep-NGF) onto matrices constructed by the phage. Using this system of ligand immobilization, matrix bound cytokines and growth factors could be delivered to cells and induce desired cell behaviors.^{13,21} The effects of the phage matrices immobilized with FGFb and NGF on rat hippocampal neural progenitor cells (NPCs) were examined. We used NPCs for our model cell culture system because of their sensitivity to biochemical cues and their environment. A schematic of our approach is shown in Fig. 1B.

We measured the specificity of the HPQ8 phage to streptavidin using ELISA binding assays and used RGD8 phage as a negative control (Fig. 2A). Different concentrations (400, 200, 100, 50 and 25 ng per well) of phages were applied onto streptavidin-coated (400 ng per well) ELISA plates and visualized using an anti-phage antibody, a secondary HRP (horseradish peroxidase)-conjugated antibody, and 3,3',5,5'-tetramethylbenzidine (TMB) substrate solution (KPL, Gaithersburg, MD). The binding assays showed that only HPQ-phage bound to streptavidin in a dose-dependent manner. We applied mixtures of HPQ8 and RGD8 at different ratios (100%, 80%, 60%, 40%, 20% and 0%, at

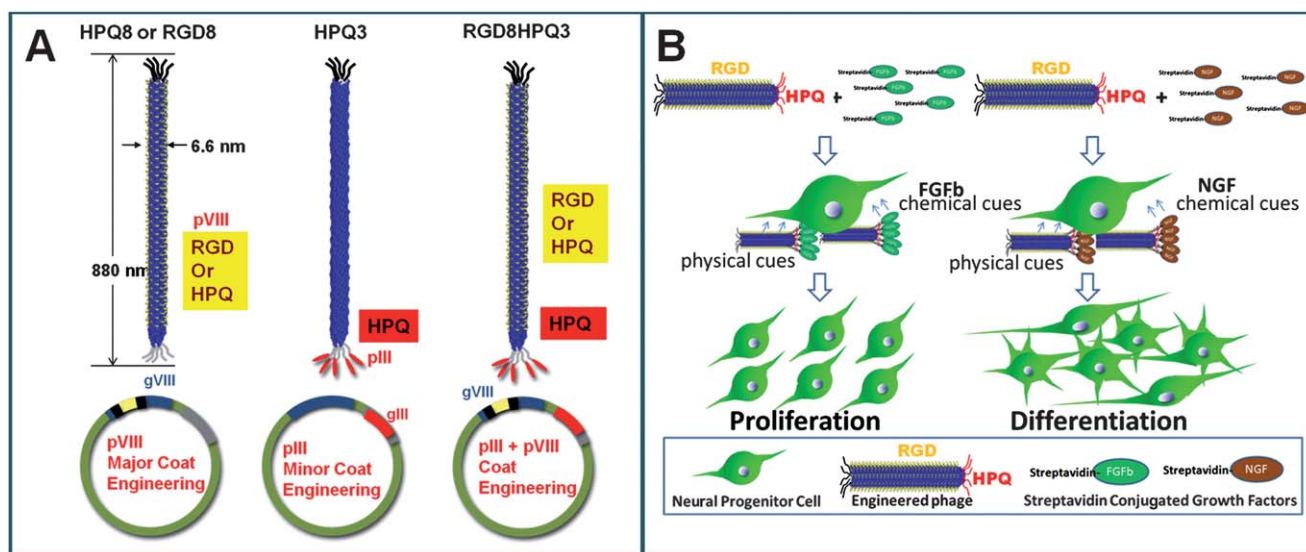


Fig. 1 Schematic illustration of the construction of multifunctional phage expressing HPQ, a biotin-like motif for directing NPC (neural progenitor cell) growth and fate. (A) We used genetically engineered M13 phages that displayed HPQ on either pVIII and/or pIII and further functionalized the major coat proteins with RGD-integrin binding motifs. (B) Strategy for immobilizing streptavidin-linked FGFb or NGF on our genetically engineered phage for directing NPC proliferation or differentiation.

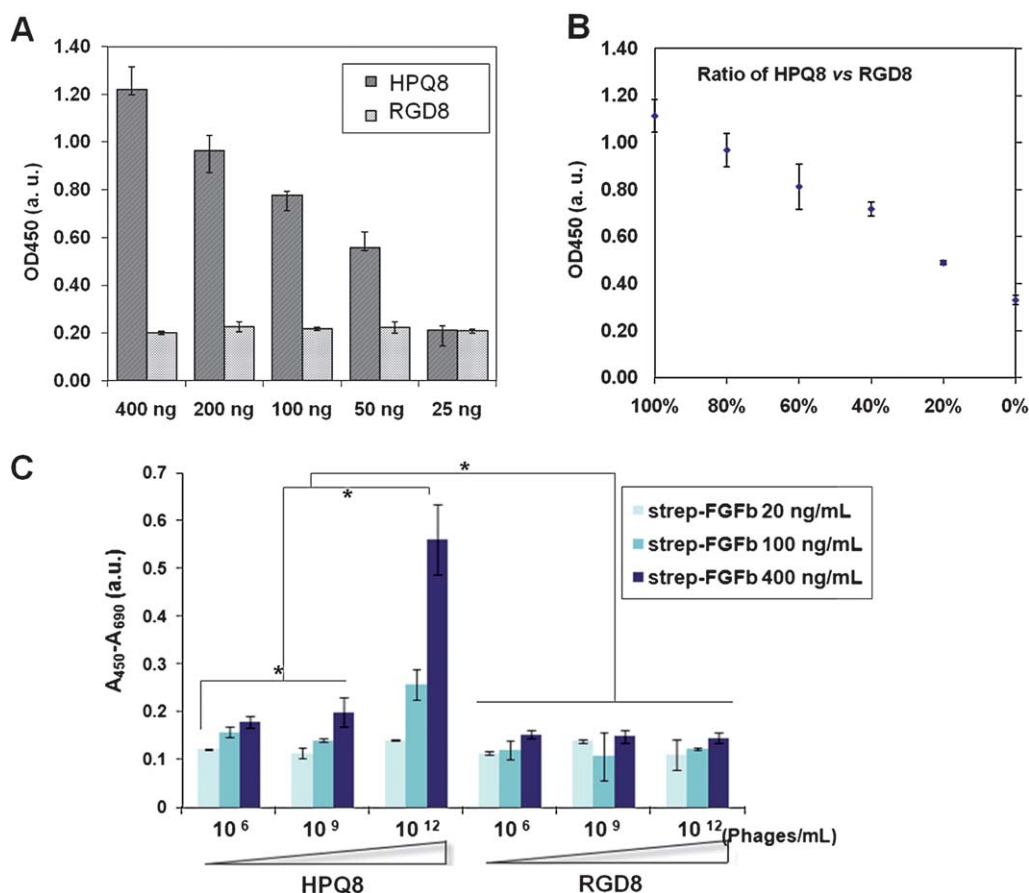


Fig. 2 Characterization of biotin-like (HPQ) peptides on the coat proteins of M13 phage. (A) Streptavidin binding assay with HPQ8 or RGD8 (control). ELISA results show that phage binding to streptavidin increased with increasing concentrations of HPQ8 but was minimal with increasing concentrations of RGD8. (B) Binding to streptavidin was tested using mixtures of different ratios of HPQ8 and RGD8 and was found to be linearly dependent on HPQ8 concentration. (C) WST1 assay of NPCs grown on varying concentrations of HPQ8 or RGD8 in the presence of strep-FGFb. Proliferation was modulated by either HPQ8 concentration or strep-FGFb concentration, whereas minimal effects were produced by changing RGD8 concentration (* $p < 0.05$, two-factor ANOVA with replication). All data are shown as means \pm standard deviation (SD) of 3 independent samples.

a total of 400 ng phage per well) to the streptavidin-coated plates. We observed that the ELISA intensity profiles decreased linearly with decreasing ratios of HPQ8 to RGD8 applied (Fig. 2B). Therefore, the HPQ-peptides on the phage surfaces were active and induced specific binding of the phage to the streptavidin. Because NPCs are able to proliferate only in the presence of FGFb in media, and because withdrawal of FGFb prompts these cells to stop growing, we tested the activity of the immobilized FGFb on NPCs using a WST1 assay (Roche, Indianapolis, IN). Wells were coated with HPQ8 or RGD8 at 10^6 , 10^9 , 10^{12} phages per mL, blocked with 1% BSA (bovine serum albumin) in PBS (phosphate buffered saline), and incubated with different concentrations (20, 100, 400 ng mL⁻¹) of streptavidin-conjugated FGFb. After washing the coated substrates, the NPCs were seeded onto the wells and cultured for 8 days in basic media with no growth factors. Fig. 2C shows that cell metabolic activity increased with increasing HPQ8 and strep-FGFb concentration. However, such effects were not observed in the RGD8 samples since they could not immobilize FGFb ($p < 0.05$, two-factor ANOVA with replication). Thus, we confirmed that the HPQ-peptide expressed on the pVIII of HPQ8 phage was fully functional for binding streptavidin and that the conjugated FGFb could modulate the metabolic activity of NPCs.

We investigated the combined effects of the HPQ-expressing phage with the RGD-expressing phage. During growth, cell spreading and migration play critical roles in controlling cell morphology and are known to be affected by RGD. Therefore, we cultured the NPC cells on streptavidin-conjugated FGFb immobilized on a mixture of RGD8 and HPQ8. We observed that the NPCs spread well and proliferated on the phage matrices only when FGFb was immobilized (Fig. 3A). In contrast, when the NPCs were cultured with strep-FGFb on a mixture of wildtype-phage (phage with no modification) and HPQ8, the NPCs exhibited aggregated morphology despite the outgrowth of NPCs (Fig. 3B). These cell spreading and aggregation morphologies indicated that the matrices needed multiple components to promote the growth of cells into desired tissue morphologies. We, therefore, constructed multifunctional phage that simultaneously displayed the RGD-peptide on pVIII and the HPQ-peptide on pIII (RGD8HPQ3). We then compared the effects of the immobilized FGFb using the three sets of phage (HPQ8, HPQ3, RGD8HPQ3). We hypothesized that the expression of HPQ on pVIII (HPQ8) would promote greater metabolic activity after FGFb immobilization than HPQ expression on pIII (HPQ3) simply due to the greater number of motifs that can be expressed on the major coat (2700) compared

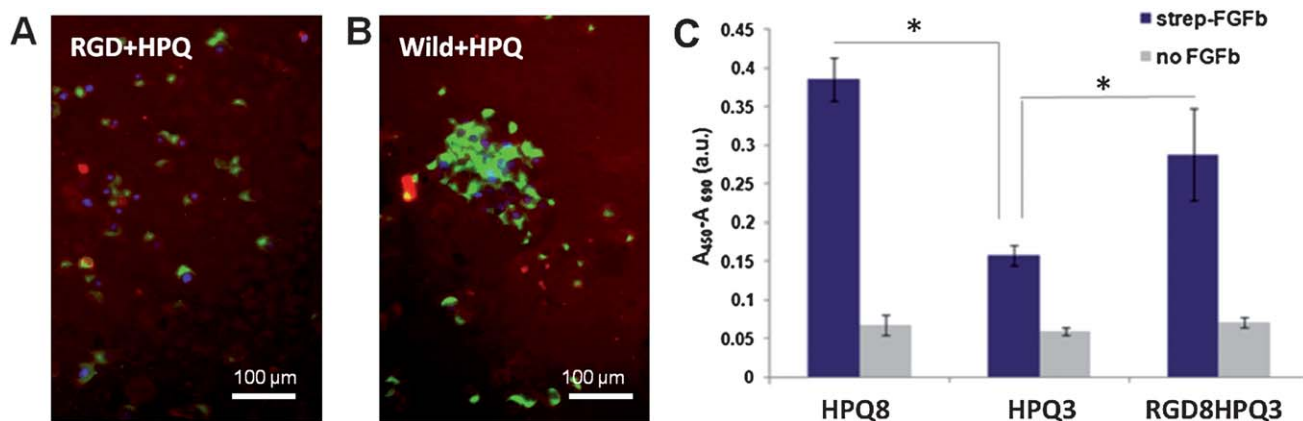


Fig. 3 Combined chemical cues presented by HPQ8 and/or RGD8. (A) NPCs cultured on a mixture of RGD8 and HPQ8. (B) NPCs cultured on a mixture of wildtype-phage and HPQ-phage. (C) WST1 assays of NPCs grown on HPQ8, HPQ3, and RGD8HPQ3 with FGFb immobilized via streptavidin (strep-FGFb concentration used: 50 ng per well). Data are shown as means \pm standard deviation (SD) of 3 independent experiments ($*p < 0.05$, single factor ANOVA).

to the minor coat (5). Interestingly, we also observed significant cellular metabolic activity when we cultured NPCs on RGD8HPQ3 with strep-FGFb (Fig. 3C) ($p < 0.05$, single factor ANOVA). Although the density of FGFb immobilized on RGD8HPQ3 was ~ 500 times lower than on HPQ8, the metabolic activity of the NPCs on RGD8HPQ3 was comparable to that of NPCs on HPQ8. We believe that the integrin binding sites provided to the cells by RGD played a synergistic role with FGFb in promoting cell spreading and proliferation.

We used these dual-functionalized phages to further control neural cell proliferation and differentiation. We coated tissue culture slides (Lab-TekII chamber slides, Nalgen Nunc International, Naperville, IL) with RGD8HPQ3, HPQ3, or HPQ8 and then linked them with strep-FGFb or strep-NGF. NPCs were then seeded onto the slides, and bright field microscopy images were taken of the NPCs after 4 days of culture (Fig. 4A). We observed that cells grown on HPQ8 in the presence of strep-FGFb showed a high degree of proliferation with cells aggregated in regions where they initially attached. Cells grown on RGD8HPQ3 with strep-FGFb were more evenly distributed due to enhanced interaction between the RGD ligands on the phage and integrin on the cell surfaces. In the presence of strep-NGF, neurite outgrowth was observed from all NPC cells on the RGD8HPQ3, HPQ8, and HPQ3 phage matrices. Neurite elongation and cell spreading were particularly enhanced on the RGD8HPQ3 sample in the presence of strep-NGF. NPC proliferation (promoted by FGFb) and differentiation (promoted by NGF) were confirmed by immunostaining with anti-*nestin* (for progenitor cells) and anti- β -tubulin III (for neural cells), respectively (Fig. 4B shows cells on RGD8HPQ3 and HPQ8). We quantified the effects of the stimulation generated by the immobilized growth factors and RGD-integrin binding peptides by characterizing parameters such as cellular distribution (cell to cell distance), cell density (number of cells per mm^2), neurite growth lengths, neurite numbers per cell, and cell aggregation (cell numbers in each aggregated cell colony) (Fig. 4C–G). The average cell to cell distances on RGD8HPQ3, HPQ3 and HPQ8 in the presence of strep-FGFb were 33.4, 22.2 and 17.7 μm , respectively (RGD8HPQ3 > HPQ3 > HPQ8) ($p < 0.05$, single factor ANOVA, $n = 25$). Similarly, in the presence of strep-NGF, the average cell to cell distances on RGD8HPQ3, HPQ3 and HPQ8 were

85.2, 35.8 and 28.1 μm , respectively ($p < 0.01$, single factor ANOVA, $n = 20$). These cell to cell distances showed that the RGD-peptide enhanced cellular spreading and distribution (Fig. 4C). Cellular densities (cells mm^{-2} ; Fig. 4D) were measured in selected areas where cells were found and are inversely related to cell to cell distances. Greater expression of HPQ induced higher cell densities in the presence of strep-FGFb (HPQ8 > HPQ3 > RGD8HPQ3), with average cell densities on RGD8HPQ3, HPQ3, and HPQ8 being 1333, 1604, and 2979 cells mm^{-2} , respectively ($p < 0.05$, single factor ANOVA, $area\ n = 3$). Cell densities in samples grown in the presence of strep-NGF exhibited similar trends. The cell densities were 250, 458, and 583 for RGD8HPQ3, HPQ3, and HPQ8, respectively ($p < 0.05$, single factor ANOVA, $area\ n = 3$). Interestingly, neurite lengths were longer in the presence of RGD (RGD8HPQ3 > HPQ3 > HPQ8) and increased with culture time (day1–day2–day4; $p < 0.05$, single factor ANOVA, $n = 8$; Fig. 4E). However, higher densities of strep-NGF binding sites increased the number of neurites formed by each cell (HPQ8 > HPQ3 > RGD8HPQ3; lower panel in Fig. 4A and F). Highly aggregated cell islands were commonly observed throughout the samples without the RGD-integrin binding peptide in samples stimulated by FGFb or NGF. In the presence of strep-FGFb, greater densities of HPQ induced higher cell counts in each colony (HPQ8 > HPQ3 > RGD8HPQ3), which increased with culture time (day1–day2–day4) ($p < 0.01$, single factor ANOVA $colony\ n = 5-22$) (Fig. 4G). We believe that the high density of binding sites for strep-FGFb and the absence of cell spreading induced the formation of highly aggregated cell island colonies in HPQ8. Therefore, the growth factors together with biochemical cues are critical for simultaneous cell spreading, cell proliferation, and differentiation. Our dual-functionalized phage (RGD8HPQ3) engineered with both RGD and HPQ motifs exhibited the morphologies that reflect both cell proliferation and differentiation.

The immobilization of growth factors and biochemical ligands on tissue matrices has become a critical issue in tissue regeneration. Various immobilization techniques have been developed using chemical or genetic modifications of the target tissue constructs.^{21,27,28} However, making these modifications without changing other chemical and physical parameters of the tissue matrices remains challenging. In our study, we demonstrated a novel strategy for

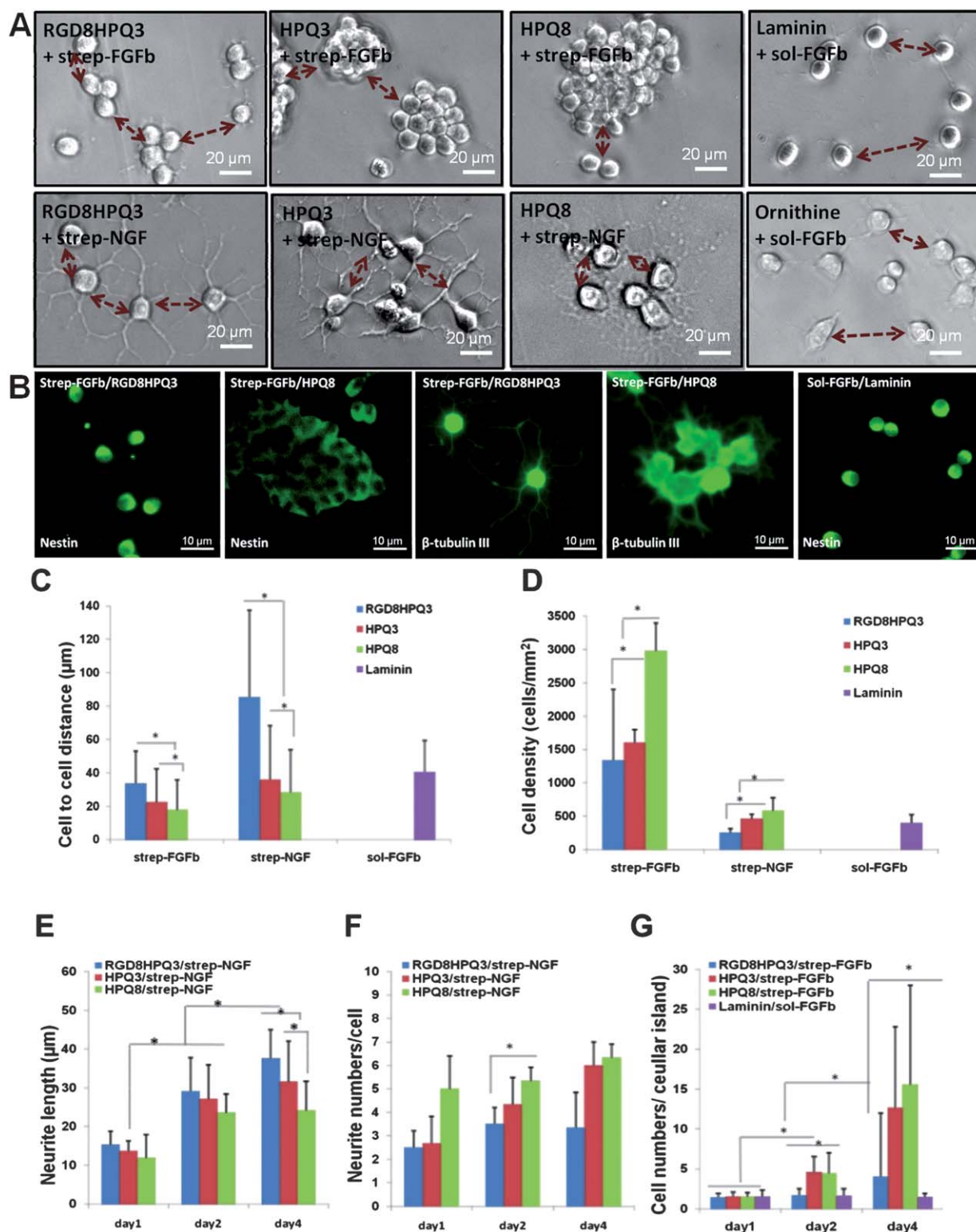


Fig. 4 Neural cell growth and fates directed by HPQ-phages. (A) NPC cells grown on RGD8HPQ3, HPQ3, and HPQ8 in the presence of strep-FGFb. Dotted arrow denotes the distribution of cells. (B) Immunostaining of NPCs grown on RGD8HPQ3 or HPQ8 with strep-FGFb or NGF, showing proliferation (by FGFb) and differentiation (by NGF). We stained for nestin (a neural progenitor cell marker) in FGFb-treated cells and for β -tubulin III (a neural cell marker) in NGF-treated cells. (C) Cell distribution, (D) cell density, (E) neurite lengths, (F) neurite numbers and (G) aggregated cell numbers were measured. Neurite lengths and neurite numbers per cell were measured in the presence of strep-NGF, and aggregated cell numbers were measured in the presence of strep-FGFb. Data are shown as means \pm standard deviation (SD). All experiments were performed in duplicate, and 4 to 5 images were taken and analyzed for each trial ($*p < 0.05$, ANOVA test).

immobilizing growth factors using M13 phage tissue engineering matrices that have been engineered to display HPQ, a biotin-analog peptide. With little change to the basic structure and function of the phage, we incorporated target growth factors onto phage matrices by simply mixing the phage with streptavidin-conjugated growth factors. In our report, we demonstrated that growth factors immobilized on phage matrices were functional (FGFb to regulate cell proliferation and NGF to regulate differentiation) and could direct cell growth towards desired cellular morphologies and fates. In addition, we constructed phages to simultaneously display RGD and HPQ and studied the combined effects of the integrin binding peptides and growth factors. The RGD8 phage provided a high density of chemical signalling (1.5×10^{13} RGD ligands per cm^2) along the nanofiber-like phage structure (880 nm by 6.6 nm), and the RGD-peptides were uniformly displayed with a spacing of 2.7 nm axially and 2 nm laterally.^{33,58} The additional expression of HPQ on the five copies of pIII on RGD8 provided a modulation-linker that could bind to various biochemical ligands, with little change to the phage. Our phage tissue matrix system can, therefore, be used as a test bed for characterizing the effects of biochemical cues using desired growth factors. Optimized densities, spacing, and presentation of growth factors and cytokines are important factors for inducing desired cellular morphologies.^{59–62} Using the RGD8HPQ3 dual-functionalized phage, we demonstrated that the combined chemical cues of RGD-integrin and growth factors are important in orchestrating desired cellular growth and morphologies.

Conclusions

We developed novel phage tissue matrices that were engineered to express biotin-like (HPQ)- and integrin binding (RGD)-peptides. The resulting HPQ-phages could be easily attached to various functional motifs through streptavidin conjugation. We demonstrated that the HPQ-engineered phage could immobilize growth factors (FGFb and NGF) while still enabling them to retain their bioactivity. Together with the phage expressing RGD-integrin binding peptide, the HPQ-phage was able to orchestrate NPC proliferation and differentiation. Our HPQ-phage system may provide a tool for studying various biochemical effects in cell biology and may be useful for developing convenient tissue matrices for engineering tissues.

Acknowledgements

We thank Professor David Schaffer for generously donating the neural progenitor cells. This work was supported by the Hellman Family Faculty Fund (SWL); start-up funds from the Berkeley Nanoscience and Nanoengineering Institute at the University of California, Berkeley (SWL); and the Laboratory Directed Research and Development fund from the Lawrence Berkeley National Laboratory.

References

- D. Gospodarowicz, D. Delgado and I. Vlodavsky, *Proc. Natl. Acad. Sci. U. S. A.*, 1980, **77**, 4094–4098.
- R. O. Hynes, *Cell*, 1992, **69**, 11–25.
- A. B. Huber, A. L. Kolodkin, D. D. Ginty and J. F. Cloutier, *Annu. Rev. Neurosci.*, 2003, **26**, 509–563.
- R. Milner and I. L. Campbell, *J. Neurosci. Res.*, 2002, **69**, 286–291.
- J. T. Rutka, G. Apodaca, R. Stern and M. Rosenblum, *J. Neurosurg.*, 1988, **69**, 155–170.
- S. F. Oster, A. Deiner, E. Birgbauer and D. W. Sretavan, *Semin. Cell Dev. Biol.*, 2004, **15**, 125–136.
- I. Shirato, Y. Tomino, H. Koide and T. Sakai, *Cell Tissue Res.*, 1991, **266**, 1–10.
- H. Makino, Y. Yamasaki and Z. Ota, *Nephron*, 1994, **66**, 189–199.
- K. Hironaka, H. Makino, Y. Yamasaki and Z. Ota, *Kidney Int.*, 1993, **43**, 334–345.
- N. R. Alexander, K. M. Branch, A. Parekh, E. S. Clark, I. C. Iwueke, S. A. Guelcher and A. M. Weaver, *Curr. Biol.*, 2008, **18**, 1295–1299.
- K. Roy, H.-Q. Mao, S. H. Lim, S. Zhang, G. Christopherson, K. Kam and S. Fischer, in *Biomaterials as Stem Cell Niche*, Springer, Berlin, Heidelberg, 2010, vol. 2, pp. 89–118.
- S. K. Powell and H. K. Kleinman, *Int. J. Biochem. Cell Biol.*, 1997, **29**, 401–414.
- J. C. Schense, J. Bloch, P. Aebischer and J. A. Hubbell, *Nat. Biotechnol.*, 2000, **18**, 415–419.
- G. A. Silva, C. Czeisler, K. L. Niece, E. Beniash, D. A. Harrington, J. A. Kessler and S. I. Stupp, *Science*, 2004, **303**, 1352–1355.
- E. Ruoslahti, *Annu. Rev. Cell Dev. Biol.*, 1996, **12**, 697–715.
- J. F. Pollock and K. Healy, in *Strategies in Regenerative Medicine*, ed. M. Santin, Springer, New York, 2009, pp. 97–154.
- R. Raghov, *FASEB J.*, 1994, **8**, 823–831.
- Neural Stem Cells for Brain and Spinal Cord Repair*, ed. T. Zigova, E. Y. Snyder and P. R. Sanberg, Humana Press, Totowa, NJ, 2003.
- R. Flaumenhaft and D. B. Rifkin, *Mol. Biol. Cell*, 1992, **3**, 1057–1065.
- F. Ramirez and D. B. Rifkin, *Matrix Biol.*, 2003, **22**, 101–107.
- Y. Ito, *Soft Matter*, 2008, **4**, 46–56.
- Y. Ito, J. Zheng, Y. Imanishi, K. Yonezawa and M. Kasuga, *Proc. Natl. Acad. Sci. U. S. A.*, 1996, **93**, 3598–3601.
- Y. Ito, J. S. Li, T. Takahashi, Y. Imanishi, Y. Okabayashi, Y. Kido and M. Kasuga, *J. Biochem.*, 1997, **121**, 514–520.
- R. L. Driessen, H. M. Johnston and S. K. Nilsson, *Exp. Hematol. (N. Y., U. S.)*, 2003, **31**, 1284–1291.
- D. E. Discher, D. J. Mooney and P. W. Zandstra, *Science*, 2009, **324**, 1673–1677.
- B. K. Mann, R. H. Schmedlen and J. L. West, *Biomaterials*, 2001, **22**, 439–444.
- T. Pompe, K. Salchert, K. Alberti, P. Zandstra and C. Werner, *Nat. Protocols*, 2010, **5**, 1042–1050.
- Y. Ito, S. Kondo, G. Chen and Y. Imanishi, *FEBS Lett.*, 1997, **403**, 159–162.
- T. Douglas and M. Young, *Nature*, 1998, **393**, 152–155.
- S. W. Lee, C. B. Mao, C. E. Flynn and A. M. Belcher, *Science*, 2002, **296**, 892–895.
- R. R. Naik, S. J. Stringer, G. Agarwal, S. E. Jones and M. O. Stone, *Nat. Mater.*, 2002, **1**, 169–172.
- C. B. Mao, D. J. Solis, B. D. Reiss, S. T. Kottmann, R. Y. Sweeney, A. Hayhurst, G. Georgiou, B. Iverson and A. M. Belcher, *Science*, 2004, **303**, 213–217.
- A. Merzlyak and S. W. Lee, *Curr. Opin. Chem. Biol.*, 2006, **10**, 246–252.
- K. T. Nam, D. W. Kim, P. J. Yoo, C. Y. Chiang, N. Meethong, P. T. Hammond, Y. M. Chiang and A. M. Belcher, *Science*, 2006, **312**, 885–888.
- D. Frenkel and B. Solomon, *Proc. Natl. Acad. Sci. U. S. A.*, 2002, **99**, 5675–5679.
- G. W. Kreutzberg, *Trends Neurosci.*, 1996, **19**, 312–318.
- S. L. Hart, A. M. Knight, R. P. Harbottle, A. Mistry, H. D. Hunger, D. F. Cutler, R. Williamson and C. Coutelle, *J. Biol. Chem.*, 1994, **269**, 12468–12474.
- V. V. Ivanenkov, F. Felici and A. G. Menon, *Biochim. Biophys. Acta, Mol. Cell Res.*, 1999, **1448**, 450–462.
- A. Hajitou, M. Trepel, C. E. Lilley, S. Soghomonyan, M. M. Alauddin, F. C. Marini, B. H. Restel, M. G. Ozawa, C. A. Moya, R. Rangel, Y. Sun, K. Zaoui, M. Schmidt, C. von Kalle, M. D. Weitzman, J. G. Gelovani, R. Pasqualini and W. Arap, *Cell*, 2006, **125**, 385–398.
- W.-J. Chung, A. Merzlyak, S. Y. Yoo and S.-W. Lee, *Langmuir*, 2010, **26**, 9885–9890.
- A. Merzlyak, S. Indrakanti and S.-W. Lee, *Nano Lett.*, 2009, **9**, 846–852.
- W.-J. Chung, A. Merzlyak and S.-W. Lee, *Soft Matter*, 2010, **6**, 4454–4459.
- S. Y. Yoo, W.-J. Chung, T. H. Kim, M. Le and S.-W. Lee, *Soft Matter*, 2011, **7**, 363.

- 44 G. P. Smith and V. A. Petrenko, *Chem. Rev.*, 1997, **97**, 391–410.
- 45 V. I. Romanov, D. B. Durand and V. A. Petrenko, *Prostate*, 2001, **47**, 239–251.
- 46 D. J. Rodi, A. S. Soares and L. Makowski, *J. Mol. Biol.*, 2002, **322**, 1039–1052.
- 47 P. C. Weber, M. W. Pantoliano and L. D. Thompson, *Biochemistry*, 1992, **31**, 9350–9354.
- 48 B. A. Katz, *Biochemistry*, 1995, **34**, 15421–15429.
- 49 B. A. Katz and R. T. Cass, *J. Biol. Chem.*, 1997, **272**, 13220–13228.
- 50 S. W. Lee, S. K. Lee and A. M. Belcher, *Adv. Mater.*, 2003, **15**, 689–692.
- 51 J. J. Devlin, L. C. Panganiban and P. E. Devlin, *Science*, 1990, **249**, 404–406.
- 52 L. B. Giebel, R. T. Cass, D. L. Milligan, D. C. Young, R. Arze and C. R. Johnson, *Biochemistry*, 1995, **34**, 15430–15435.
- 53 S. W. Lee, S. Lee and A. Belcher, *Adv. Mater.*, 2003, **15**, 689–692.
- 54 P. C. Weber, M. W. Pantoliano and L. D. Thompson, *Biochemistry*, 1992, **31**, 9350–9354.
- 55 M. A. Mclafferty, R. B. Kent, R. C. Ladner and W. Markland, *Gene*, 1993, **128**, 29–36.
- 56 E. Engel, A. Michiardi, M. Navarro, D. Lacroix and J. A. Planell, *Trends Biotechnol.*, 2008, **26**, 39.
- 57 J. M. Goddard and J. H. Hotchkiss, *Prog. Polym. Sci.*, 2007, **32**, 698–725.
- 58 S. Y. Yoo, W. J. Chung, T. H. Kim, M. Le and S. W. Lee, *Soft Matter*, 2010.
- 59 S. P. Massia and J. A. Hubbell, *J. Cell Biol.*, 1991, **114**, 1089–1100.
- 60 G. Maheshwari, G. Brown, D. Lauffenburger, A. Wells and L. Griffith, *J. Cell Sci.*, 2000, **113**, 1677–1686.
- 61 C. S. Chen, M. Mrksich, S. Huang, G. M. Whitesides and D. E. Ingber, *Science*, 1997, **276**, 1425–1428.
- 62 J. V. Shah, *J. Cell Biol.*, 2010, **191**, 233–236.